Indian Journal of Chemical Technology
Vol. 24, March, 2017 pp. 153-161

Thermo-structural analysis of sol-gel route based yttria stabilized tetragonal zirconia (YSTZ) powders for thermal barrier applications

Dipak Kumar*,[1] & K N Pandey[2]

[1,]Mechanical Engineering Department, Raj Kumar Goel Institute of Technology Ghaziabad 201 003, India
[2]Mechanical Engineering Department, Motilal Nehru National Institute of Technology Allahabad, Allahabad 211 004, India
E-mail: dipakmnnit@gmail.com

Received 14 July 2015; accepted 25 August 2016

Yttria stabilized zirconia (YSZ) powders have been synthesized via sol-gel solution route in order to obtain thermal barrier coatings (TBCs) from sol-gel. Conventional method of preparation of sol and gel has been used for coating and thermal analysis respectively. Prepared gel is heated at 150°C for 3h and 250°C for 3 h and thermal analysis of powder is carried out. At this stage two routes are followed to get the sintered powder. Sintered powder-1 is obtained after heat treatment of 800°C for 3 h and sintered powder-2 is obtained by heat treatment at 1300°C for 3 h. Thermal analysis of both gel and dried powder at 150°C for 3 h show the exothermic process of 187.5°C, indicating the start of the nucleation process of crystallization of the tetragonal phase of YSZ powder. Sintered powder obtained after heating the powder at 1300°C for 3 h is found to have more identical grain size distribution of YSZ powder in comparison to powder sintered at 800°C for 3 h. The total mass loss of gel and powder obtained by drying gel at 150°C for 3 h is found to be 31.4% and 31.0% respectively, indicating amorphous behavior at this stage.

Keywords: Characterization, Sol-gel techniques, Thermo-structural analysis, Yttria stabilized zirconia (YSZ)

With the increase in more powerful and efficient engines, it requires to increase the operating temperature and decrease in thermal conductivity of the thermal barrier coatings (TBCs) for protecting and maintaining the base metal of the engine. The most suitably used ceramic material for insulating is yttria stabilized zirconia (YSZ) because of structural hardening behavior during cooling in the meta-stable tetragonal t-phase[1,2]. There are two dry-routes TBC deposition techniques, namely air plasma spraying (APS) and electron beam-physical vapor deposition (EB-PVD). They give quite different microstructures of deposited TBCs. APS give a lamellar microstructures with a low thermal conductivity in the range of 0.7-1.1 $Wm^{-1}K^{-1}$, which is twice lower than EB-PVD based coatings having columnar orientation. EB-PVD based coatings give the best mechanical performance than that of APS based coatings[2-6]

The conventional EB-PVD and Plasma sprayed methods are directional, costly and complicated. An alternate to these processes is a chemical sol-gel route which is non-directional and easy to apply at temperature much lower than conventional coating processes[7,8].

The aim of the present paper is to characterize the as-prepared YSZ powder obtained by two sintering methods. In the first method YSZ gel was first heated at 150°C and 250°C for 3 h to get dried powder and then again heat treated at 800°C for 3 h. This sintered powder was called sintered powder-1. In the second method, dried YSZ powder obtained by heating the gel at 250°C for 3 h was heat treated at 1300°C for 3 h. The main goal was to compare the structural and morphological properties of YSZ powders obtained by above mentioned two methods, so as to get a simpler method of getting YSZ powder for TBC applications.

To get the nature of prepared sol-gel, thermal analysis of the gel and powder was done. Further, characterization of sol-gel and its derived powder was done using Thermo Gravimetric Analysis (TGA), Differential Thermal Analysis (DTA) and Differential Scanning Calorimetry (DSC) and compared with X-ray diffraction (XRD). XRD data was then compared with Transmission Electron Microscopy (TEM), High Resolution Transmission Electron Microscopy (HR-TEM). Morphology of powders was analyzed through Scanning Electron Microscopy (SEM), Field Emission-Scanning Electron Microscopy (FE-SEM), TEM and HR-TEM.

Experimental Section

Materials

Precursors used for the yttria stabilized zirconia powder were zirconium (IV) propoxide ($Zr(OPr)_4$) (M/s Sigma Aldrich), yttrium (III) nitrates hexahydrate ($Y(NO_3)_3.6H_2O$) (M/s Alfa Aesar), 1-propanol solvent (M/s SRL), acetyl acetone (M/s SRL) as a complexing agents and water used as hydrolysis agents.

Synthesis of Sol-gel

Sol-gel technique is based on the hydrolysis and condensation of metal alkoxides, M (OR)x, where M^{z+} is a metal, and 'R' an alkyl group (R= Methyl, Ethyl, Propyl,…). Starting precursor zirconium propoxide is a transition metal alkoxide, that is, highly sensitive to moisture. The sensitiveness of zirconium propoxide is principally due to its tendency to increase its coordination number up to 7 or 8. To avoid any reactivity of fast hydrolysis of alkoxide with water or moisture, synthesis must be performed under controlled environment. The aim of the synthesis was to make 5 g powder of 7 wt.% yttria stabilized zirconia (ZrO_2.7wt.%Y_2O_3). Molecular weight of $ZrO_2.7Y_2O_3$ is 149.026. For 5 g powder of 7YSZ, 0.533 g of $7Y_2O_3$ was required and for 0.533 g of $7Y_2O_3$, 2.29 g of $Y(NO_3)_3.6H_2O$ was used. Accordingly, 16.8 g of $Zr(OPr)_4$ solution was taken. The method of preparation of sol-gel is presented in flow chart 1(a). As zirconium propoxide is sensitive to moisture, Acetyl acetone (AcAc) was first mixed with 1-propanol to avoid any uncontrolled reactions.

Powder preparation

After the gelation at 60°C, gel samples were dried at 150°C and 250°C for 3 h in an oven to obtain a dried-gel by simple evaporation of the solvent. Then, resulting dried gels were sintered at 800°C and 1300°C with heating rate of 2.5°C/min for 3 h and then it were cooled to room temperature. The powders sintered at 800°C were called sintered powder-1 and that at 1300°C will be called sintered powder-2. The sintered powders were then grinded separately by hand grinder to obtain crystallized yttria stabilized zirconia powder.

Powder characterization

The crystallographic structures of sol-gel based YSZ powders were characterized by X-ray diffraction measurements. The patterns were measured at room temperature with Rigaku Smart Lab diffractometer. Copper radiation was used as the x-ray source ($\lambda(CuK\alpha_1)$ = 1.5406Aº; $\lambda(CuK\alpha_2)$ = 1.5444Aº; K_β = 1.3922Aº) with Ni filter. Generator setting was 30 mA and 40 kV. To study the phase crystallization evolution, the sintered powder-1 and sintered powder-2 were placed in a platinum crucible. The specimens were scanned continuously in 2θ range of 20º-70º with scan step time of 19.4 seconds and step size 2θ of 0.019º. The average crystalline size of the powder particles was determined by the Scherer formula (assuming no micro-strains) given by Equation (1).

$$D = 0.9\lambda / FWHM \cos\theta \quad \ldots (1)$$

where λ= 0.15405 nm, FWHM is the full width at half maximum of the peaks; and θ is the diffraction angle. Average crystalline size was found to be 0.003271 nm at 800°C and 0.012906 nm at 1300°C.

Phase analysis was also carried out by an X-Ray Diffractometry (XRD) with diffraction angles (2θ) ranging between 20-80°, by a scanning rate of 0.04°/min.

The crystal structure of powder samples at 800°C and 1300°C calcination temperatures were determined by a TEM, HR-TEM (JEM 2100, make JEOL Japan) operated at 200 kV and selected area electron diffraction (SAED). In addition, average grain sizes and the agglomerated morphology of two different sintered particles were also examined by TEM, and Field Emission Scanning Electron Microscopy (FESEM). TEM samples were prepared by putting YSZ powder suspended in ethanol on a carbon-coated copper mesh grid, then drying in air at room temperature. For FESEM, the particles were dropped on a carbon stub. After drying, the powders were coated in Gold-Palladium plasma coating unit.

Thermal analysis

Thermal analysis of YSZ gel prepared after heating the YSZ composite sol at 60°C as shown in Fig. 1a and its derived powder samples prepared after drying the gel at 150°C for 3 h and 250°C for 3 h (Fig. 1b) were carried out using thermo gravimetric analysis (TGA) coupled with differential thermal analysis (DTA)/differential calorimetry (DSC) (Model: Diamond, TG/DTAN) in nitrogen gas atmosphere with a heating rate of 20°C/min. Thermal analysis was done to study the weight loss and heat loss-heat gain with the increase in temperature. Alumina was taken as reference materials for thermal analysis.

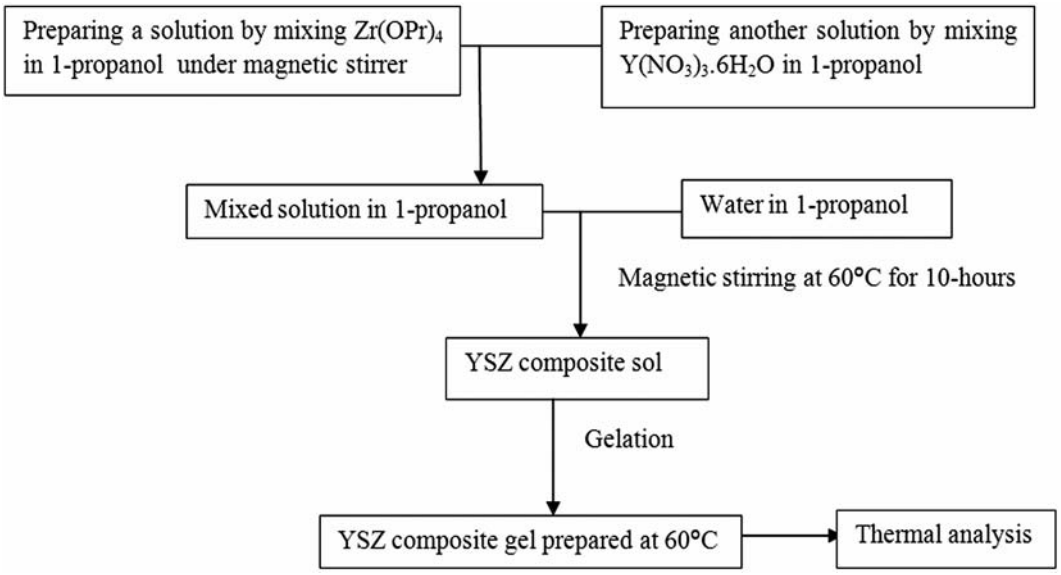

Fig. 1(a) — Procedure for YSZ sol-gel synthesis.

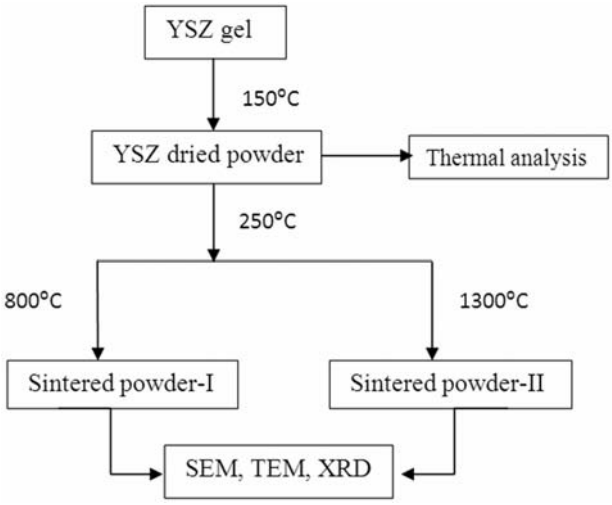

Fig. 1(b) — Drying routes of YSZ gel.

Results and Discussion

XRD analysis

Effect of temperature

The diffraction pattern of the YSZ powder samples annealed at 150°C show only wide bands (no peaks) within 20°-40° and very wide bands within 40°-65°, which is a typical behavior of unstructured or amorphous material. As the calcination temperature increases, metastable tetragonal phase (JCPDS No.080-4130) begins to nucleate into crystal at 250°C annealing temperature and wide bands become narrow as shown in Fig. 2 (reflection at 26.54°). XRD of conventional powder is also shown in Fig. 2. XRD pattern of sintered powder-1 matches the pattern of conventional YSZ powder in tetragonal form. Atomic planes and their phases of sintered powder-1 were investigated through JCPDS No.016-2095, while that of sintered powder-2 through 016-2095, 080-4130, 037-1484[7] and 070-1431. Tetragonal phase of conventional YSZ powder was investigated through JCPDS No. 016-2095 and 065-9024. Figure 2 presents XRD patterns of the phase transformation of YSZ powders with the increase in temperature upto 1300°C. No peak was found for the powder obtained by drying the gel at 150°C for 3 h (Fig. 1b) similarly when it was heated to 250°C, no strong peak was visible. For sintered powder-1(when dried powder

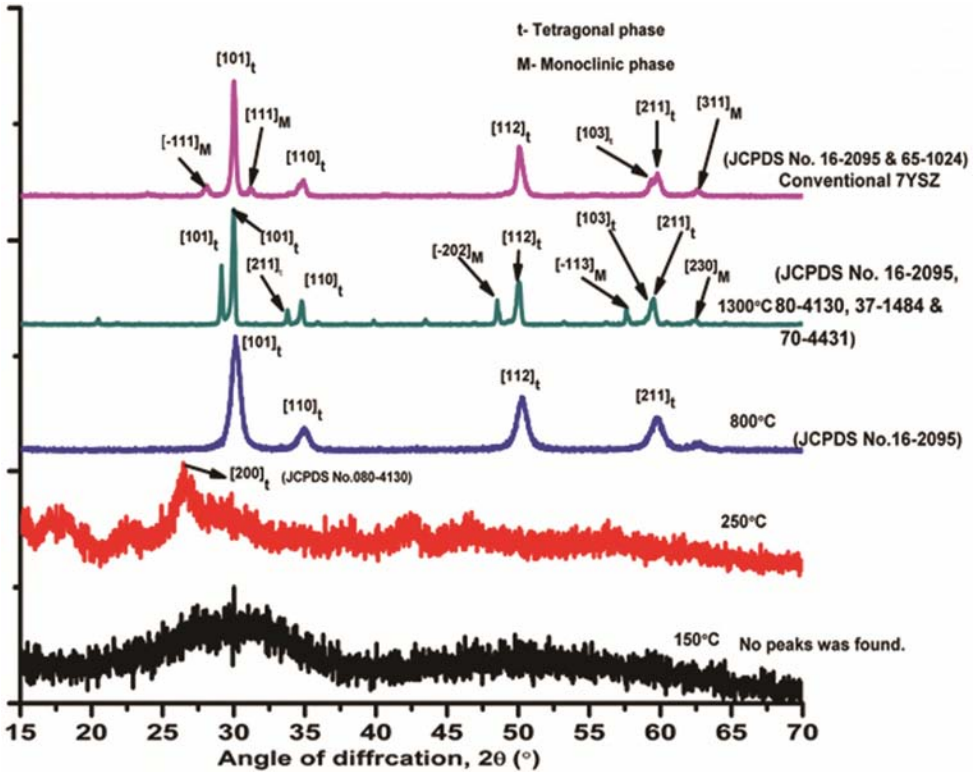

Fig. 2 — XRD pattern with variable temperature.

was annealed at 800°C for 3 h) multiple, physically powerful diffraction peaks were visible. These peaks are $[101]_t$ at 30.088º, $[110]_t$ at 34.85°, $[112]_t$ at 50.03°, $[211]_t$ at 59.54°. For sintered powder-2 (when dried powder was annealed at 1300ºC for 3 hours) some other strong diffraction peaks were also visible to $[101]_t$ at 29.07°, $[211]_t$ at 33.77°, $[-202]_M$ at 48.53°, $[-113]_M$ at 57.67°. In addition to the strong peaks, some weak light diffraction peaks are also visible for sintered powder-2. These are $[103]_t$ at 54.45°, and $[230]_M$ at 62°. Peaks are more broadened in case of sintered powder-1, indicating that crystallite size of YSZ is fine.

To discriminate the tetragonal and cubic phase from XRD patterns of Fig. 2, the patterns were further studied in the range of 70° to 80° and are presented in Fig. 3. Splitting of peaks was observed at [004] and [220] indicating only tetragonal phase for sintered powder-1 and sintered powder-2. These findings are similar to the literature[7] but contrary to literature[9,10].

Microstructure analysis

Selected area electron diffraction (SAED) analysis was used to further examine the powder phase content of sintered powder-1 and sintered powder-2. Figure 4a shows selected area electron diffraction patterns of the sintered powder-1. The [110] plane in Fig. 4a is

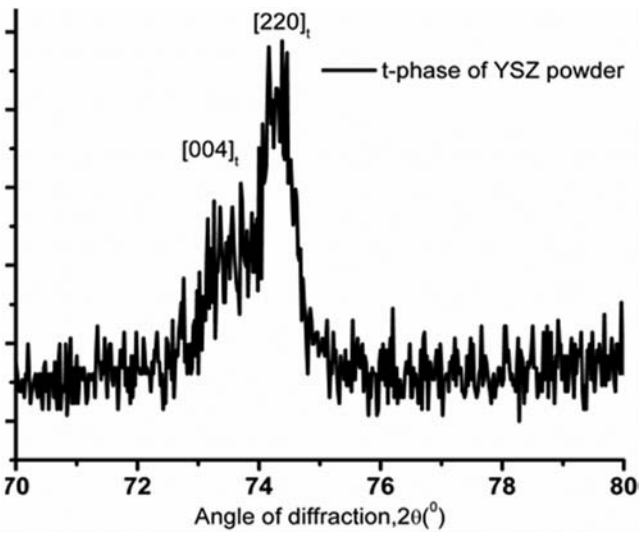

Fig. 3 — XRD pattern of YSZ pattern from 70 - 80°.

not clearly visible. It is due to low intensity peak in XRD pattern of Fig. 2. The $[101]_t$ and $[112]_t$ planes are clearly distinguishable from SAED pattern as per peak intensities of XRD pattern. In Fig. 4b, only one atomic orientation is observed. This atomic plane gives the constant lattice inter-planar distance of 2.951A° corresponding to the highest intensity of peak, indicating the presence of only tetragonal phase.

Therefore, SAED pattern clearly distinguishes the cubic and tetragonal phases in comparison to XRD patterns. Figure 4c shows the bright field image of agglomerated particles. It shows the presence of nano grain size particles at 800°C. Figure 4d confirms the elemental composition of YSZ powder particles. It also confirms yttrium as dopant in zirconium. Figure 4e shows the distribution of average particle size. The best fitting curve of average grain size distribution was obtained by using the Gaussian equation as given below:

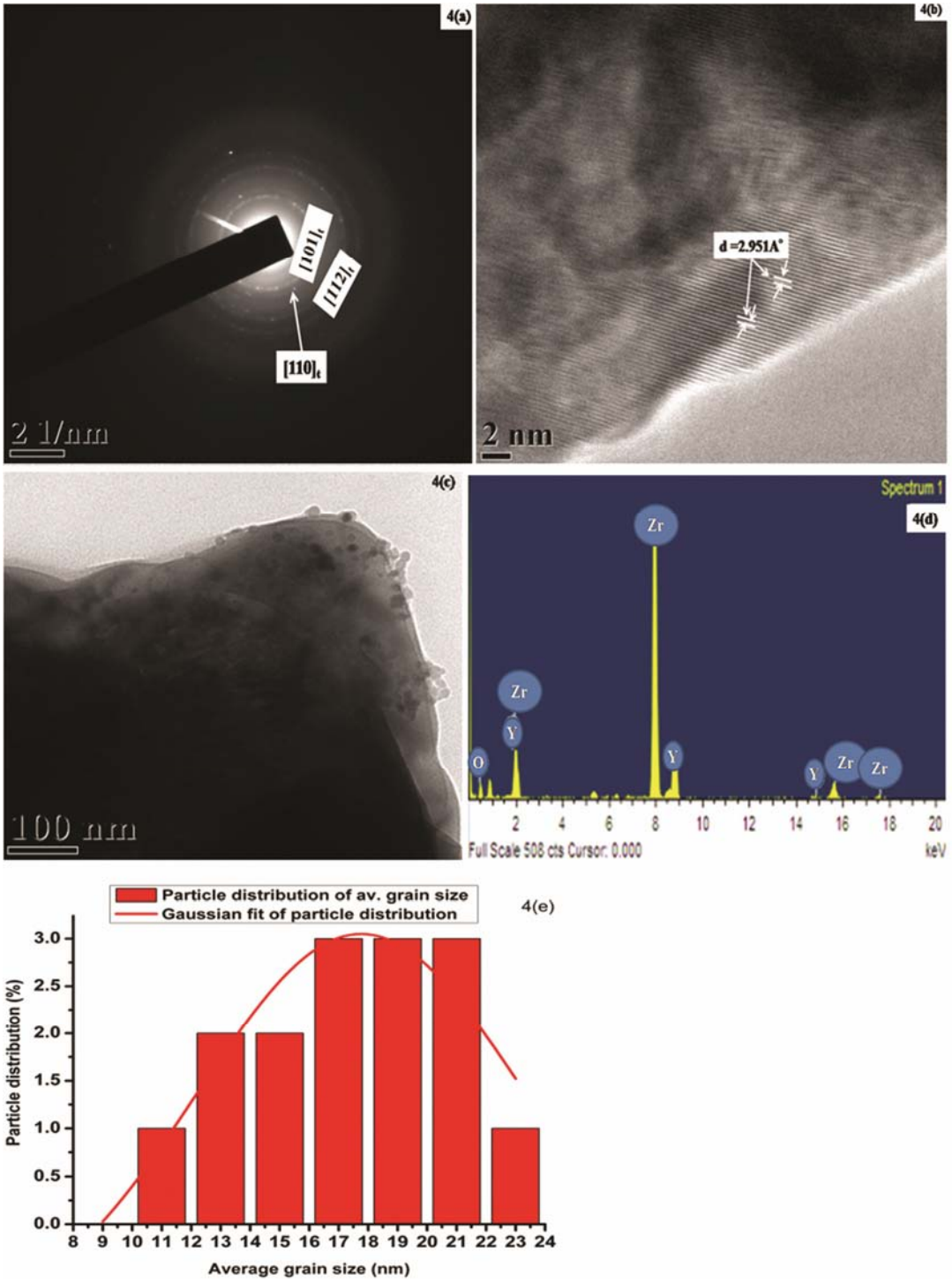

Fig. 4 — TEM image of sol-gel YSZ powder obtained after heating at 800°C for 3 h (a) SAED pattern; (b) HR-TEM images; (c) Bright field image; (d) EDX pattern and (e) Particle size distribution histogram.

$$y = y_0 + \left(\frac{A}{w\sqrt{PI/2}} \right) * \exp\left(-2 * \left(\frac{x - x_c}{w^2} \right) \right) \quad \ldots(2)$$

where x is weight function, y is independent parameters, w is full width half mean (FWHM), PI is principal intensity of grain distribution (in terms of height) and y_0, A and x_c are constants. The TEM image of sintered powder-1 is shown in Fig. 4c. It shows that the particles are almost spherical or irregular spherical with average grain size in the range of ~10 to ~24 nm. Grains grow only upto 24 nm for sintered powder-1. Grain size in the range of 8 to 29 nm shows the stable tetragonal phase[11,12].

Figure 5a shows the SAED pattern of sintered powder-2. Tetragonal YSZ lattices with inter-planar spacing of 2.951A° corresponding to the crystallographic plane of [101] are observed. 2.951A° lattice spacing show highest intensity of diffraction planes at 30.08° in Fig. 2. Second circular spots show [110] plane of tetragonal phase at 35.16°. This confirms the light intensity peak shown in XRD pattern of Fig. 2 for sintered powder-2. Third diffraction ring on TEM image shows high intensity of peaks, correspondence at 50.19° diffraction angle. The inter-planar spacing of 2.951A° in HR-TEM image of Fig. 5b distinguishes tetragonal phase from cubic phase. The TEM image shown in Fig. 5c indicates that the particles are almost spherical or irregular shape with particle size distributions having the mean diameters in the range of ~ 20 nm to ~70 nm. Particle distribution of different composition is shown in Fig. 5d. Distribution of YSZ powder particle, Fig. 5e, shows more grain growth with the increase in annealing temperature as compared to grain size distribution shown in Fig. 4e for sintered powder-1. Although unsymmetrical grain growth of particle size was also observed at 1300°C calcined temperature as compared to 800°C calcined temperature. Unsymmetrical grain growth of particle size can be observed in Fig. 5c also for sintered powder-1 for which annealing temperature was 800°C. A Gaussian best fit curve for unsymmetrical average grain growth of particle using Eq. (1) is also shown in Fig. 5e. Further, hydrostatic stresses resulting from the mixture of tetragonal and monoclinic phase and hard aggregation tendencies of particles is responsible for improving the stability of tetragonal dominated phase of YSZ synthesis[13].

Increase of monoclinic phase at 1300°C calcined temperature (Sintered powder-2) was also observed with the major amount of tetragonal phase. Exhibition of some monoclinic phase in tetragonal phase at 1300°C calcined powder may be resulted from increase of grain size with temperature[14]. Leoni *et al.*[15] reported that the tetragonal phase might be transformed into monoclinic phase upon cooling if the grain size of particles is above 1 μm. Results obtained in present analysis show that the grain size lies within the range of 20 to70 nm which is very far away from critical size of 1μm.

Shape of the grains of sintered powder-1 and sintered powder-2 are presented in the form of FESEM images in Fig. 6a and Fig. 6b, respectively. At 1300°C calcined temperature (sintered powder-2), high density of particles are observed with shape of the grains either pentagonal or hexagonal. FESEM image of sintered powder-2 (calcined temperature of 1300°C) shows better coalescence of powder grains, as well as densification and very much reduced porosity, showing better sintering aptitude. On the other side, the FESEM images of sintered powder-1(calcined temperature of 800°C) show more porosity, and therefore, sintering aptitude for powder is not better. The correlation between XRD pattern, TEM, FESEM and SEM examination express that both sintered powder 1 and 2 are not polycrystalline particles but sintered powder-2 is agglomeration of very fine particles. Grain size of this powder is also more or less uniform in comparison to sintered powder-1. However, some pores are visible in the grain boundary. Powder porosity is assumed to result from the liberation of unstable (i.e. volatile) components such as NO_2 from $Y(NO_3)_3.6H_2O$ and CO_2 from $Zr(OPr)_4$ at high calcined temperature[14], since volatile components and carboxylic groups are very sensitive to temperatures.

Thermal analysis

Thermal analysis of YSZ composite gel (Fig. 1a) and dried powder obtained by heating YSZ gel at 150°C for 3 h (Fig. 1b) was carried out to study the nucleation stage of crystalline formation with respect to temperature. For this, differential scanning calorimetry (DSC), differential thermal analysis (DTA) and thermo-gravimetric analysis (TGA) were carried out between room temperature and 1100°C[15] for powder dried at 150°C. For gel, thermal analysis was carried out between room temperature and 700°C[8] . The DTA/DSC and TGA of powder dried at

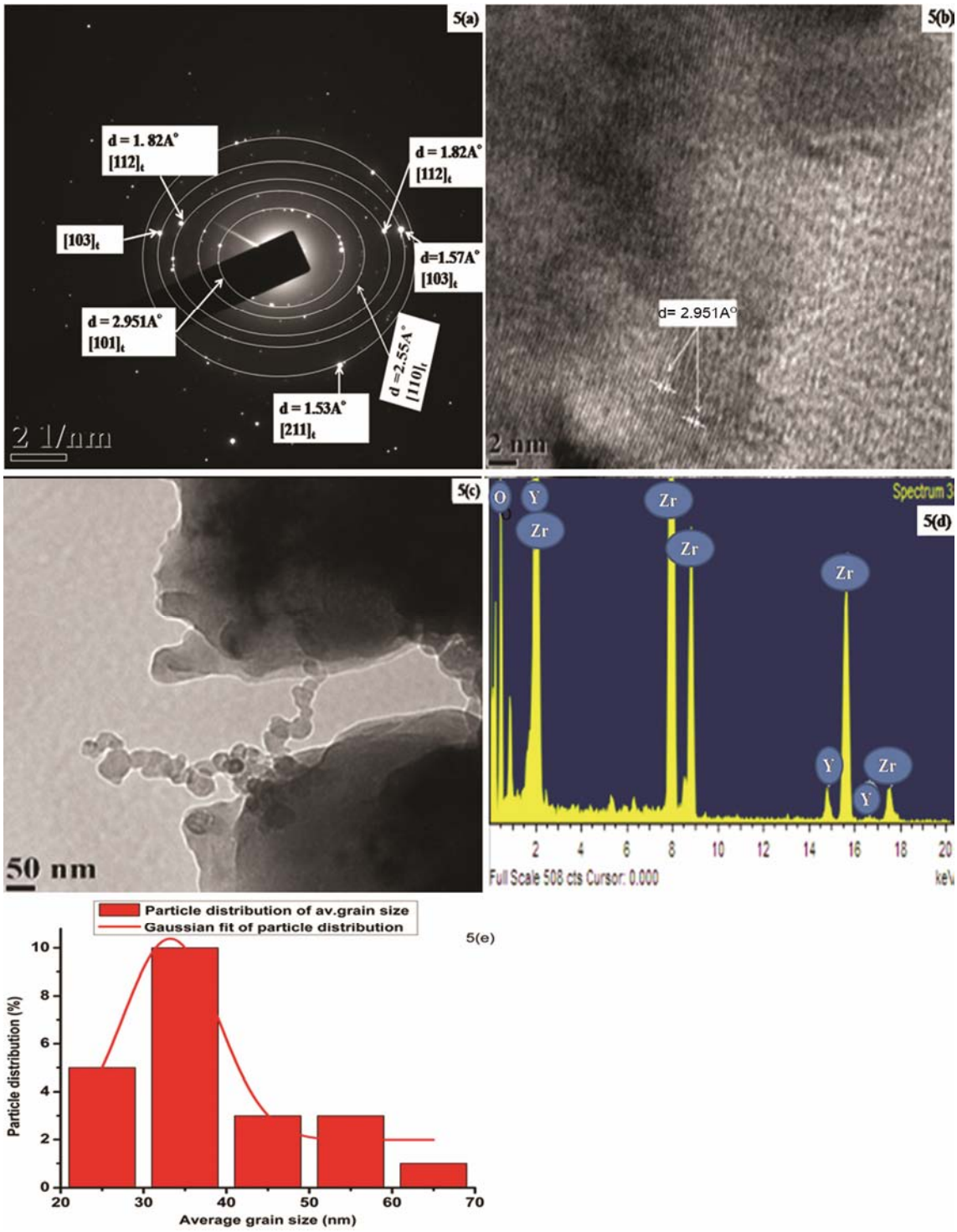

Fig. 5 — TEM image of sol-gel based YSZ powder obtained after heating at 1300°C for 3 h (a) SAED pattern; (b) HR-TEM images; (c) Bright field image; (d) EDX pattern and (e) Particle distribution of average grain size.

150°C Fig. 1(b), and YSZ composite gel are presented in Fig. 7(a) and 7(b) respectively. Both for YSZ dry powder and YSZ gel, thermal analysis was carried on three samples to verify the results. Same natures of curves were obtained for all three samples for both the cases. An endothermic peak of DSC and DTA at around 118°C was found which may correspond to the evaporation of the remaining organic and inorganic

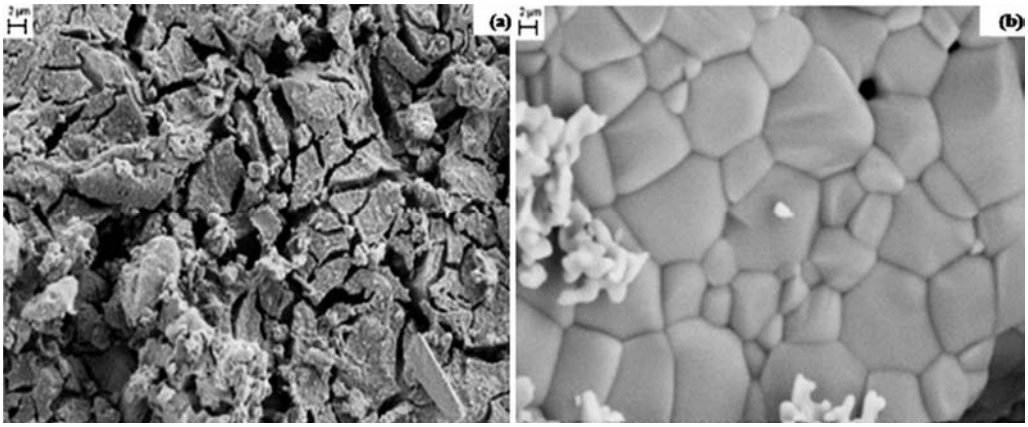

Fig. 6 — FESEM image of sol-gel YSZ powder obtained after heating at (a) 800°C for 3 h and (b) 1300°C for 3 h.

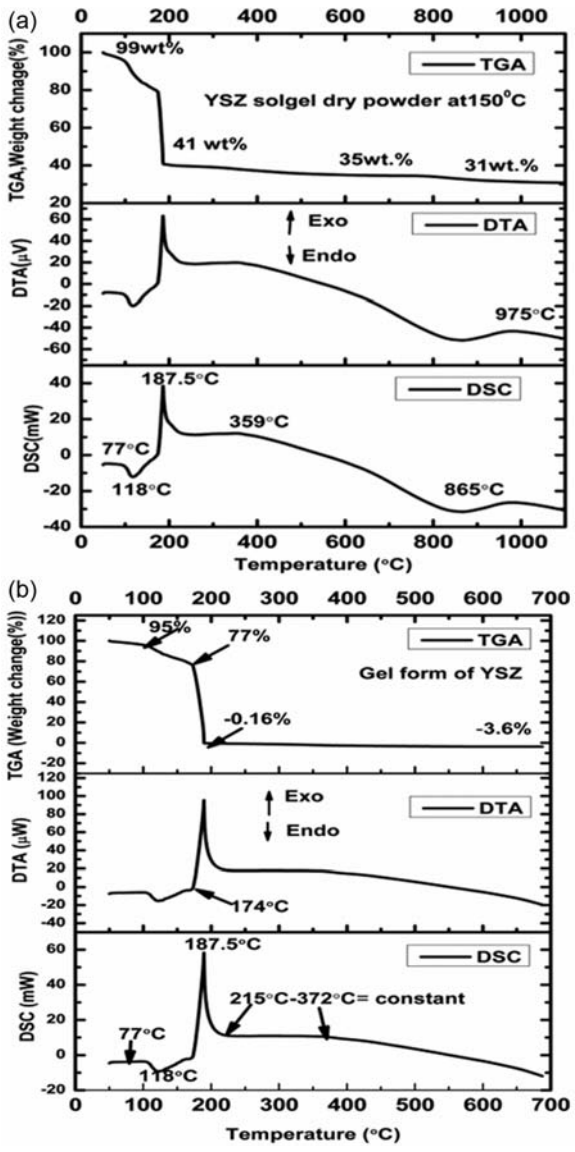

Fig. 7 — Thermal analysis curve of (a) YSZ dry powder obtained after heating at 150°C and (b) YSZ gel form.

solvent (i.e. water). A strong exothermic peak was observed at 187.5°C and can be recognized to the flaming of organic compounds and creation of crystallized zirconia[17-19]. A transition of exothermic reaction was observed around 359°C. No other thermal effect was recognized before 865°C. At around 865°C, very wide endothermic reaction was observed and at around 975°C, exothermic reaction was observed. Thereafter, no other thermal effect was obtained. Recognition of transition effect at 865°C and 975°C attributed to cooling down, that's why neither endo-nor exothermic peaks were observed. The results of DSC and DTA of dry powders may point toward the phase stability stage around 215°C-372°C, Fig. 7 (b).

Upto 77ºC, around 99% weight gain phenomena took place for both the cases. During endothermic process at 118°C, 85% weight gain was observed. At 174°C, 67% weight gain was recorded. During strong exothermic transition, weight gain was recorded upto only 33% for dry powders, while weight loss was recorded 0.16%. It can be said that the continuous desorption and remaining 1-propanol solvent release process can be divided into four steps. The main mass loss (22%) is between room temperature and 174°C. A second major mass loss of 36% (~40) is observed between 174°C and 187.5°C during endothermic to exothermic phase. This decrease of weight is because of the decomposition of transition metal bonds between $Zr(OPr)_4$ and corresponding yttrium nitrates with 6 moles of water as ligands[20,21]. Third mass loss of 6% was observed between 200°C and 800°C for dry powder samples is associated with further decomposition and flaming of the intermediate carboxylic products (i.e. from chelating agents) due

to pyrolysis nature[20]. The final mass loss of 4% is also observed which corresponds to the formation of H_2O by some condensation stage of surface-OH groups. This indicates the nucleus formation of the tetragonal phase. The difference of mass loss in dry powder and gel samples is about 0.4%. The initial negative value of weight change (Fig. 7b) for gel indicates dehydration of gel below 250°C. This weight loss corresponds to endothermic reaction and is due to the adsorption of organic-inorganic solvent and dehydration of gels[22]. The weight loss of 0.16% is too small to responsible for the exothermic reaction. Powder diffraction of gel heating at and above 800°C confirms crystallization of the amorphous gel to tetragonal zirconia.

Conclusion

Homogeneous 7 weight% Y_2O_3 containing yttria stabilized zirconia (7YSZ) is synthesized with optimum amount of starting chemical precursors and controlling the sol-gel route parameters. Calcination temperature of 800°C and 1300°C is chosen on the basis of exhibited suitable crystallinity and phase properties. Calcined powders at temperatures 800°C and 1300°C consist of big agglomeration of nano-particles. Although, better grain growth of particles with identical grain size are found at 1300°C calcined temperatures. [101]atomic plane, maximum 2.951A° of inter-planar spacing, controlled particle's grain size ~1μm (maximum) with increase of temperature, earlier splitting of [220] atomic plane into [004] at 73° diffraction angle and angle of diffraction in the range of ~30° - ~30.13° at highest intensity is found to be critical characteristic for the presence of predominantly tetragonal phase.

The total mass loss is compared to the initial mass is of around 31% for powder and 31.4% for gels. The DSC/DTA analysis coupled with TGA and XRD, indicated that the exothermic processes at 187.5°C can be related to the nucleation process of crystallization of tetragonal YSZ. Typical TGA and DTA/DSC results show that the gel and powder samples are continuously dehydrated in a long temperature range, between room temperature and 700°C for gel and room temperature and 1100°C for powder.

Acknowledgement

The authors acknowledge the testing facilities of XRD and SEM provided by Center for Interdisciplinary Research (CIR) MNNIT, Allahabad.

The financial support provided by TEQIP-II at MNNIT Allahabad is also highly acknowledged.

References

1 Lelait L, Alperine S, Diot C & Mevrel M, *Mater Sci Eng A*, 120-121 (1989) 475.
2 Kumar D, Pandey K N & Das D K, *Proc I MechE PartL:J Mat: Des Appl*, 2016, Doi:10.1177/1464420716640570.
3 Jiang X, Liu C & Lin F, *J Mater Sci Technol*, 23 (2007) 449.
4 Klemens P G & Gell M, *Mater Sci Eng A*, 245 (1998) 143.
5 Cao X Q, Vassen R & Stover D, *J Eur Ceram Soc*, 24 (2004) 1.
6 Clarke D R & Phillpot S R, *Mater Today*, 8 (2005) 22.
7 Viazzi C, Bonino J P & Ansart F, *Surf Coat Technol*, 201 (2006) 3889.
8 Fenech J, Viazzi C, Bonino J P, Ansart F & Barnabe A, *Ceram Int*, 35 (2009) 3247.
9 Tan D, Lin G, Liu Y, Teng Y, Zhuang Y, Zhu B, Zhao Q & Qiu J, *Nanopart Res*, 13 (2011) 1183.
10 Lamas D G, Rosso A M & Anzorena M S, *Scripta Mater*, 55 (2006) 553.
11 Lamas D G, Fuentes R O & Fabregas I O, *J Appl Cryst*, 38 (2005) 867.
12 Garvie R C, *J Phys Chem*, 82 (1978) 218.
13 Kazemi F, Saberi A, Malek Ahamadi S, Sohrabi S, Rezaie H R & Tahriri M, *Ceramics*, 55 (2011) 26.
14 Shukla S & Seal S, *Int Mater Rev*, 50 (2005) 45.
15 Leoni M, Jones R L & Scardi P, *Surf Coat Technol*, 108-109 (1998) 107.
16 Hua Z, Wang X M, Xiao P & Shi J, *J Europ Ceram Soc*, 26 (2006) 2257.
17 Salehi S & Fathi M H, Ceram Int, 36 (2010) 1659.
18 Suciu C, Gagea L, Hoffmann A C & Mocean M, *Chem Engng Sc*, 61 (2006)7831.
19 Wen T L, Hebert V, Vilminot S & Bernier J C, *J Mater Sc*, 26 (1991) 3787.
20 Abakeviciene B, Zalga A, Tautkus S, Pilipavicius J & Navickas E, *Soild State Ionics*, 225 (2012) 73.
21 Kim S G, Nam S W, Yoon S P, Hyun S H, Han J, Lim T H & Hong S A, *J Mater Sc*, 39 (2004) 2683.
22 Kaliszewski M S & Heuer A H, *J Am Ceram Soc*, 73 (1990) 1504.